

Glass-transition behavior of Ni: Calculation, prediction, and experimentDmitri V. Louzguine-Luzgin,^{1,2,a)} Rodion Belosludov,² Masatoshi Saito,³ Yoshiyuki Kawazoe,² and Akihisa Inoue^{1,2}¹WPI Advanced Institute for Materials Research, Tohoku University, Sendai 980-8577, Japan²Institute for Materials Research, Tohoku University, Sendai 980-8577, Japan³Faculty of Medicine, School of Health Sciences, Niigata University, Niigata 951-8518, Japan

(Received 1 May 2008; accepted 3 November 2008; published online 23 December 2008)

Vitrification of metals and alloys has received much attention in the field of materials science. Although some progress has been made, this phenomenon has yet to be fully understood. Herein, we investigate the vitrification process of pure Ni using an *ab initio* molecular dynamics simulation. The results of the molecular dynamics simulation and predictions from the specific volume and density diagrams as well as a casting experiment indicate that Ni may have a high reduced glass transition temperature but due to kinetic reasons is not a good glass former. The results of the present work provide new information about the glass-transition phenomenon and suggest that the reduced glass transition temperature is only an indicator of how easily can glass be formed and that its stability is a significantly more important feature. © 2008 American Institute of Physics.

[DOI: 10.1063/1.3042240]

I. INTRODUCTION

Upon sufficiently fast cooling, crystallization of the liquid phase is suppressed and the liquid solidifies to produce a glass¹—a disordered solid-state substance, which is also often called an amorphous solid. The liquid-glassy trace exhibits continuity, and the specific volume of a crystal at a given temperature is lower than that of the glassy phase^{2,3} provided that the substance contracts upon solidification. The glass-transition phenomenon has attracted significant attention from physicists and materials scientists.^{4,5} Upon a glass transition, the average relaxation time has been reported to change by a few orders of magnitude from 0.1 to 100 s. This change is directly manifested by a rapid decrease in the heat capacity C_p from liquid to solid values as the degrees of freedom become kinetically frozen.⁶ The glass transition temperature T_g can be defined as the onset temperature of the C_p increase upon heating.⁷ Notwithstanding the significant progress achieved in the field, a comprehensive theory of glass transition has yet to be developed.

The increase in the glass-transition temperature (T_g) with the cooling rate indicates a kinetic character of vitrification⁸ because the relaxation process⁹ is not as efficient at a high cooling rate. However, although Kauzmann¹⁰ has clearly illustrated the thermodynamic aspects of a glass transition when the entropy of a liquid approaches that of a crystal, it is likely that both kinetic and thermodynamic aspects of the glass transition are important. The role of thermal conductivity has also been discussed recently.¹¹ It is generally thought that pure metals must have low glass-transition temperatures due to their low glass-forming ability (GFA).

Because the synthesis of a metallic amorphous phase in an Au–Si system by a rapid solidification technique was successful,¹² numerous metallic amorphous and glassy alloys

have been produced up to date. The high GFA achieved at some alloy compositions has allowed bulk metallic glassy alloys to be produced in a thickness range of 1–100 mm using various casting processes.^{13,14} Metallic glassy alloys exhibit high strength, hardness, and wear resistance as well as a large elastic deformation, good soft magnetic properties, and high corrosion resistance.^{13–15}

The thermal expansion of metals occurs due to the anharmonicity of the potential energy well, and at constant pressure it exhibits a nonlinear behavior.^{16,17} The thermal expansion of liquid metals is found to differ from that of solids. According to recent studies, the thermal expansion of liquids is due to an increase in the free volume of holes,¹⁸ and for many metals a nearly linear density variation as a function of temperature has been observed^{19,20} even upon deep supercooling.²¹ The thermal expansion of the glassy phase has been studied by *in situ* x-ray diffraction measurement.²² In addition, we have approached the glass-transition temperature from the viewpoint of specific volume versus temperature diagram,²³ extended the criterion of a small volume change upon melting, which was proposed previously,^{24,25} and introduced the δ parameter. The δ parameter indicates how fast a metal/alloy can reach the glass transition temperature. Ni and some noble metals such as Pt and Pd theoretically exhibit high reduced glass-transition ($T_{rg} = T_g/T_1$) temperatures (T_g —glass-transition temperature, T_1 —equilibrium liquidus temperature) due to the relatively high T_1 , small volume changes upon solidification, and sufficient thermal expansion coefficients of the liquid phase. Pt- and Pd-based alloys are also among the best glass formers.^{15,26}

II. CALCULATIONS AND EXPERIMENT

In the present work, we investigated the vitrification process of pure Ni by an *ab initio* molecular dynamics (MD) simulation method at an extremely high cooling rate of

^{a)} Author to whom correspondence should be addressed. Electronic mail: dml@imr.tohoku.ac.jp. Tel.: +81 (22) 215-2592. FAX: +81 (22) 215-2381.

10^{13} K/s, which is higher than the predicted critical cooling rate, estimated T_g , and compared it to the equivolume temperature obtained from the specific volume versus temperature diagram. Because the thermal expansion coefficient of a liquid phase (α_l) is higher than that of a solid one (α_s), the specific volume of certain metals in a liquid state at a sufficiently low temperature may be less than that of the corresponding solid one^{3,27} upon cooling if crystallization is suppressed.²⁸

We calculated and plotted the volume changes in a solid crystalline and a liquid phase for pure Ni as a function of temperature starting from solid Ni at 298 K (8.9 Mg/m^3) and liquid Ni at 1727 K (7.905 Mg/m^3) using thermal expansion data. If the specific volume-temperature plots of a liquid and the corresponding solid crystalline phase intersect at a temperature above absolute zero, this intersection temperature may be treated as a critical temperature (equivolume temperature). Then if the metal contracts upon solidification and nucleation of the crystal is suppressed, the liquid may become a glassy phase above this temperature at a sufficiently high cooling rate. By analogy with Kauzmann's paradox,¹⁰ we suggest that a liquid metal should not have a lower volume at a given temperature than its crystalline counterpart provided it contracts upon solidification and changes in the chemical bond character do not occur.

The volume coefficient of thermal expansion $\alpha(T)$ at constant pressure is

$$\alpha = \left(\frac{1}{V_0} \frac{\partial V}{\partial T} \right)_p, \quad (1)$$

where V is the specific volume at a given temperature T .

The following equation allows the specific volume of solid Ni V_s at a given temperature to be calculated:

$$V_s = V_0 + \alpha_s(T)V_0(T - T_0). \quad (2)$$

The thermal expansion coefficient of liquid Ni (α_l) (which is essentially constant) can be derived from the density (ρ_l) variation as a function of temperature

$$\rho_l = \rho_m - \alpha_l \rho_m (T - T_m), \quad (3)$$

where ρ_m is the density of a liquid Ni measured at 1727 K, which is close to the melting temperature (T_m).

To estimate Kauzmann temperature (T_K) (Ref. 10) of pure Ni, we used the entropy data from Ref. 29 which in turn uses heat capacity (C_p) data for crystalline Ni below³⁰ and above 298 K,³¹ as well as that of liquid Ni.³² The heat capacity value for liquid Ni was $43.1 \pm 1.3 \text{ J/mol K}$.

In order to record a cooling curve, a cylindrical rod sample of pure Ni with a 3 mm diameter was cast by a copper mold Ar injection casting technique (pressure 0.7 MPa) in an argon atmosphere at a nearly ambient pressure. The time-temperature cooling curve was obtained by recording the temperature of the melt with a thin (0.3 mm diameter) K-type thermocouple, which was connected to an analog-to-digital signal converter (Graphtec GL-500). Data were sampled in 1 ms intervals.

The initial structure of liquid pure Ni was constructed using the reverse Monte Carlo simulation method³³ and the density values as well as pair distribution function (PDF)

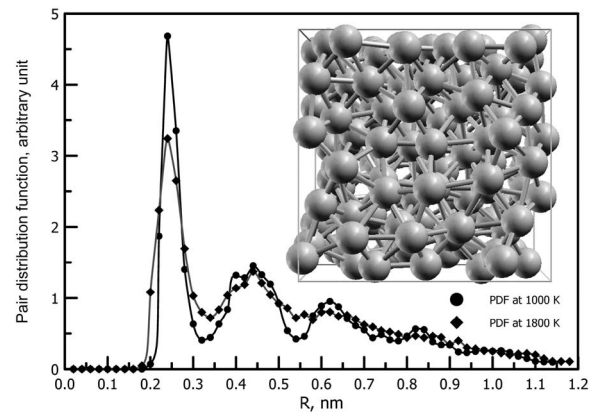


FIG. 1. PDFs of liquid and glassy Ni at 1800 and 1000 K, respectively. The inset shows a bulk Ni supercell at 1000 K.

were obtained elsewhere.³⁴ A cubic cell consisting of 128 particles ($1.167 \times 1.167 \times 1.167 \text{ nm}^3$) was created using a PDF of pure Ni at 1800 K, and then this cell was used as the initial configuration in further calculations.

The supercooling process was calculated using the *ab initio* MD simulations. All MD calculations were performed using the Vienna *ab initio* simulation package³⁵ within the local spin density approximation. Vanderbilt ultrasoft pseudopotentials³⁶ were used and a plane-wave cutoff energy of 241.7 eV was applied. The quenching rate used to obtain the glass was 10^{13} K/s. For this purpose, beginning from 1800 K (the cell size was corrected for this temperature) the structure was cooled for each 100 K during 2000 time steps where each time step was 5 fs. After each 100 K decrement, the change in density was corrected by an additional volume relaxation calculation with a higher cutoff energy of 302 eV. Due to the large supercell and numerous time steps, the MD simulation was performed on the G point only.

Because density functional methods always have errors in volume calculations and this study used a minimal number of k -points, we performed the volume optimization for a bulk Ni supercell ($3 \times 3 \times 3$) structure (Fig. 1, inset) with an initial lattice constant $a = 1.0572 \text{ nm}$, which equals the experimental one within the same input parameters described previously. The calculated lattice constant for the selected supercell was found to be 1.0285 nm. This difference in the calculated and experimental lattice constants allowed us to fit our simulation results.

III. RESULTS

Figure 1 shows the resulting PDFs, which illustrate a nonperiodic structure. Some features of these PDFs are quite remarkable. As the temperature decreased, as expected, the first peak became stronger and sharper, whereas the second peak was split into two shoulders. The PDF had a tendency to not become asymptotical to one because the size of the supercell is limited. One can see that the sample at 1000 K possessed a much higher degree of short and medium range order than that at 1800 K (Fig. 1).

Figure 2(a) exhibits the specific volume-temperature (V - T) diagram created for pure Ni in accordance with the data found in Refs. 16, 17, and 21. Different literature

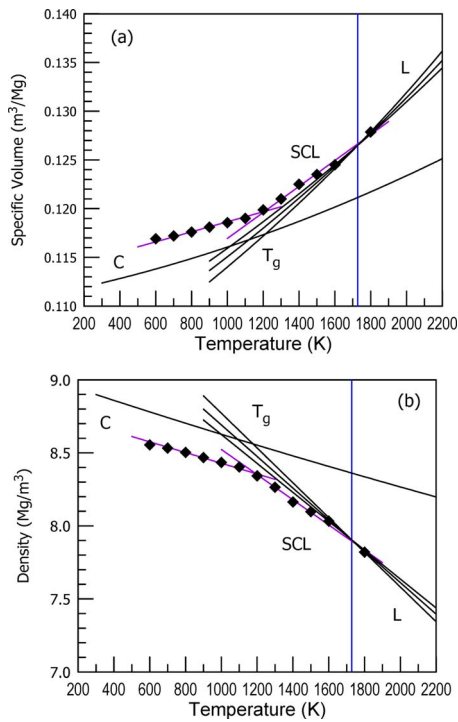


FIG. 2. (Color online) (a) Specific volume-temperature and (b) density-temperature diagrams for pure Ni (solid lines) in a liquid (according to different literature sources) and solid state. Diamond points and two least-squares method fits represent the results of the *ab initio* MD simulation. Vertical line indicates the melting temperature.

sources provide slightly different thermal expansion coefficients for liquid Ni. The specific volume of liquid V_l at a given temperature was calculated from the corresponding density values ρ_l . The same diagram for density versus temperature is shown in Fig. 2(b). Recent levitation experiments have shown that the constancy of the thermal expansion coefficient of liquid Ni obtained by density measurements is maintained even below the liquidus temperature.²¹ The V - T and ρ - T diagrams plotted in Fig. 2 allowed the theoretical equivolume temperature for Ni to be determined as about 0.57–0.7 ($T_1^{\text{Ni}} = 1728$ K) via the intersection point of two V - T and ρ plots obtained for the solid and liquid states. This value is very high for a pure metal.

Figure 2 also shows the *ab initio* MD simulation results. A few interesting features are found. First, the slope of the liquid Ni curve differed from that calculated by the thermal expansion coefficient, which was obtained at a slow cooling. Such a difference can be explained considering the extremely high cooling rate of 10^{13} K/s used during the MD simulation as required to avoid crystallization of liquid Ni. Hence, it is reasonable to assume that at such a high cooling rate, the changes in the atomic configurations in a liquid cannot follow the changes in temperature due to the relatively large relaxation time^{14,37} of such a liquid, which causes the dV/dT slope to deviate from the predicted slope using the thermal expansion coefficient.

The slope of the curve calculated using *ab initio* MD simulation changes around 1100–1200 K followed that of solid Ni at lower values of the specific volume and higher density. This temperature corresponds well to that obtained

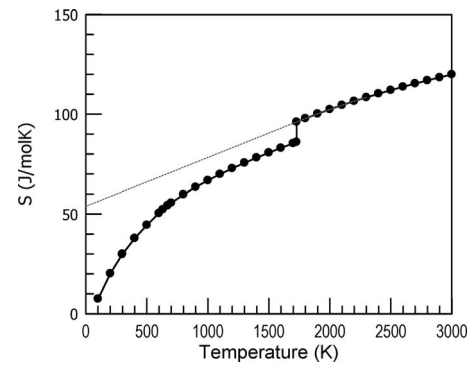


FIG. 3. Entropy values of solid and liquid Ni as a function of temperature (Refs. 29–33). Dotted line represents extrapolation of $S_l(T)$. Equilibrium solidus-liquidus temperature is 1728 K.

using the thermal expansion data of solid and liquid Ni calculated for slow cooling of the liquid phase and heating of solid crystalline Ni. Thus, 1150 K may be considered as the vitrification temperature of Ni. Because the thermal expansion coefficients of Ni measured by different authors differ,^{14,16,21} the vitrification temperature predicted by the thermal expansion data may differ by about 100 K.

Figure 3 shows the variation in the entropy of pure Ni in solid [$S_s(T)$] and liquid states [$S_l(T)$] as a function of temperature. Because the intersection point was difficult to determine, the $S_l(T)$ values obtained by integrating $C_p(T)$ could be imprecise, which may significantly influence T_K .

Figure 4 shows the cooling curve recorded on Cu mold casting of pure Ni in an argon atmosphere. The deflection of the temperature curve from exponential cooling related to the beginning of crystallization occurred near 1350 K. A significant change simultaneously occurred in the derivative dT/dt (the cooling rate) near 1200 K. Thus, Ni shows a high supercooling of about 380 K.

IV. DISCUSSION

As long as heterogeneous nucleation is suppressed, Ni exhibits deep supercooling even at a slow cooling rate. Moreover, the self-diffusion coefficient of Ni in liquid Ni, $\text{Ni}_{80}\text{P}_{20}$, $\text{Pd}_{40}\text{Ni}_{40}\text{P}_{20}$, and $\text{Pd}_{43}\text{Ni}_{10}\text{Cu}_{27}\text{P}_{20}$ alloys over a wide temperature range varies only within 10%–20% as a function of composition. Pure Ni at 1795 K has a self-diffusion coefficient of $3.80 \pm 0.06 \times 10^{-9}$ $\text{m}^2 \text{s}^{-1}$, which is only 20% be-

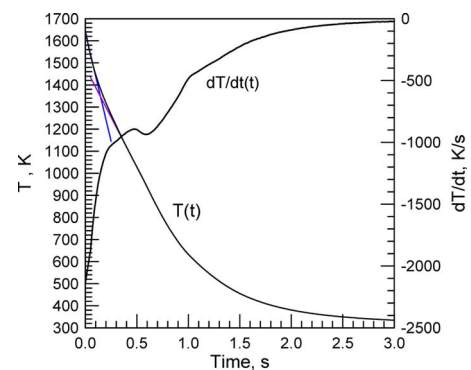


FIG. 4. (Color online) Cooling curve recorded on Cu mold casting of pure Ni. Resultant rod sample has a crystalline structure.

low the diffusion coefficients of Ni in Ni–P and Pd–Ni–Cu–P alloys.³⁸ Moreover, it has also been shown that diffusive motion is governed by the packing fraction of the atoms, which is similar to dense liquids.³⁸ Furthermore, it has been emphasized³⁸ that Ni, Ni₈₀P₂₀, Pd₄₀Ni₄₀P₂₀, Pd₄₀Ni₁₀Cu₃₀P₂₀, and Pd₄₃Ni₁₀Cu₂₇P₂₀ (Refs. 39 and 40) are all densely packed^{41,42} liquids with very similar values for the packing fraction.⁴³ It should be mentioned that according to Ref. 44 a certain amount of glassy Ni, which contains impurities, has been reported to form in local thin areas upon splat cooling at a cooling rate of 10¹⁰ K/s. As amorphous Ni can be produced by gas condensation,⁴⁵ it is assumed that T_K may be higher than suggested in Fig. 3, but the precise value is difficult to calculate. Moreover, as found in Ref. 3, T_g of Pd₄₃Cu₂₇Ni₁₀P₂₀ obtained by the enthalpy change is very similar to that produced using thermal expansion data of solid and liquid.

Thus, if Ni has such a high reduced glass transition temperature and its self-diffusion coefficient follows the same trend for various different glass-forming alloys, why is Ni not a bulk glass former? This question can be answered by considering competing crystalline compounds⁴⁶ and packing efficiency.^{47,48} In bulk glass-forming alloys, the competing phase is rarely a primary pure metal phase but is a supersaturated solid solution, an intermetallic compound, or a quasicrystal^{49,28} in which the formation mechanism may differ. The formation of such a phase often requires long-range diffusion while a pure metal crystallizes by a polymorphous transformation mechanism. On the other hand, equal sized spheres prefer crystalline fcc or hcp structures to fill the space. These are the reasons why monoatomic metallic glasses are highly unstable even below T_g . Moreover, this instability is also indicated in the empirical principles, which determine the GFA of alloys.^{13,15} Thus, even after vitrification at an extremely high cooling rate (say at gaseous-phase condensation) monoatomic metallic glasses can devitrify/crystallize for kinetic reasons^{50,51} upon heating within a short time span. Even the Au–Si binary glassy alloy was quite unstable.¹² Hence, instability limits the usage of T_{rg} as well as the proposed δ criterion concept to estimate the GFA of alloys. Thus, the importance of stability of the supercooled liquid ($\Delta T_x = T_x - T_g$, where T_x is the onset crystallization temperature)⁵² or $\gamma = T_x / (T_g + T_1)$ criterion⁵³ [as well as the γ_m (Ref. 54) and other similar criteria] should be emphasized. Moreover, the glass-transition temperature of some amorphous alloys is above the crystallization temperature (at a certain heating rate),⁵⁵ and even if these alloys possess sufficiently high T_{rg} values, the thermal stability of the resultant glass is not high.

Another aspect which should be discussed is fragility of the liquid.^{9,56} A parameter F_1 introduced recently considers both T_{rg} and the fragility index $m = d \log_{10} \tau / d(T_g/T) |_{T=T_g}$ of the supercooled liquid (τ is the Maxwell relaxation time).⁵⁷ It has been suggested that the parameter T_{rg} alone is a good GFA indicator for glass forming systems with similar fragility values but is not reliable for materials with significantly different fragilities.⁵⁷ Pure metals are believed to be fragile liquids. Thus, even if some of them have high T_{rg} , their actual GFA is not high.

V. CONCLUSIONS

The equivolume temperature approach to determine the glass-transition temperature of metals and *ab initio* MD simulation demonstrate that T_{rg} of Ni may be as high as ~ 0.6 – 0.7 , which is an extremely high value for pure metals. The above result limits the applicability of the T_{rg} concept to metallic glasses and indicates that a parameter combining both T_{rg} and the stability of the supercooled liquid against crystallization must be used. In addition, our finding provides new insight in the investigation of the glass-transition phenomenon. Moreover, it also suggests that Ni may be a suitable base and alloying element for bulk glassy alloys.

ACKNOWLEDGMENTS

This work was partially supported by a Grant-in-Aid “Priority Area on Science and Technology of Microwave-Induced, Thermally Non-Equilibrium Reaction Field” (Grant No. 18070001) by the Ministry of Education, Sports, Culture, Science and Technology of Japan. The authors sincerely thank Mr. T. Saito from Tohoku University for his assistance in casting the Ni sample.

- ¹D. Turnbull, *Contemp. Phys.* **10**, 473 (1969).
- ²P. G. Debenedetti and F. H. Stillinger, *Nature (London)* **410**, 259 (2001).
- ³I.-R. Lu, G. P. Goerler, H. J. Fecht, and R. Willnecker, *J. Non-Cryst. Solids* **312–314**, 547 (2002).
- ⁴A. Van den Beukel and J. Sietsma, *Acta Metall. Mater.* **38**, 383 (1990).
- ⁵D. Turnbull and M. H. Cohen, *J. Chem. Phys.* **52**, 3038 (1970).
- ⁶T. G. Fox and P. J. Flory, *J. Appl. Phys.* **21**, 581 (1950).
- ⁷A. L. Greer, *Science* **267**, 1947 (1995).
- ⁸H. S. Chen, *Rep. Prog. Phys.* **43**, 353 (1980).
- ⁹C. A. Angell, *Science* **267**, 1924 (1995).
- ¹⁰W. Kauzmann, *Chem. Rev.* **43**, 219 (1948).
- ¹¹D. V. Louzguine-Luzgin, A. D. Setyawan, H. Kato, and A. Inoue, *Philos. Mag.* **87**, 1845 (2007).
- ¹²W. Klement, R. H. Willens, and P. Duwez, *Nature (London)* **187**, 869 (1960).
- ¹³A. Inoue, *Mater. Trans., JIM* **36**, 866 (1995).
- ¹⁴W. L. Johnson, *MRS Bull.* **24**, 42 (1999).
- ¹⁵A. Inoue, *Acta Mater.* **48**, 279 (2000).
- ¹⁶*Smithells Metals Reference Book*, 8th ed., edited by W. F. Gale and T. C. Totemeier (Elsevier, New York, 2004), p. 14-1.
- ¹⁷Y. S. Touloukian, *Thermophysical Properties of Matter: Thermal Expansion, Metallic Elements and Alloys* (Plenum, New York, 1975), pp. 1–100.
- ¹⁸V. G. Bar'yakhtar, L. E. Mikhailova, A. G. Ilinski, A. V. Romanova, and T. M. Khristenko, *Sov. Phys. JETP* **68**, 811 (1989).
- ¹⁹S. Saito, Y. Shiraishi, and Y. Sakuma, *Trans. Iron Steel Inst. Jpn.* **9**, 118 (1969).
- ²⁰S. Watanabe, *Trans. Jpn. Inst. Met.* **12**, 17 (1971).
- ²¹J. Brillo and I. Egry, *Int. J. Thermophys.* **24**, 1155 (2003).
- ²²D. V. Louzguine-Luzgin, A. Inoue, A. R. Yavari, and G. Vaughan, *Appl. Phys. Lett.* **88**, 121926 (2006).
- ²³D. V. Louzguine-Luzgin and A. Inoue, *J. Mater. Res.* **22**, 1378 (2007).
- ²⁴A. R. Yavari, *Phys. Lett. A* **95**, 165 (1983).
- ²⁵A. Inoue, T. Negishi, H. M. Kimura, T. Zhang, and A. R. Yavari, *Mater. Trans., JIM* **39**, 318 (1998).
- ²⁶H. S. Chen, *Acta Metall.* **22**, 1505 (1974).
- ²⁷D. V. Louzguine, A. R. Yavari, K. Ota, G. Vaughan, and A. Inoue, *J. Non-Cryst. Solids* **351**, 1639 (2005).
- ²⁸D. V. Louzguine-Luzgin and A. Inoue, *J. Nanosci. Nanotechnol.* **5**, 999 (2005).
- ²⁹<http://www.chem.msu.su/rus/tsiv/Ni/ivtan0000.html>.
- ³⁰R. H. Busey and W. F. Giaque, *J. Am. Chem. Soc.* **74**, 4443 (1952).
- ³¹I. Barin, *Thermochemical Data of Pure Substances*, 3rd ed. (Wiley, New York, 1997), p. 1.
- ³²P. D. Desai, *Int. J. Thermophys.* **8**, 763 (1987).
- ³³R. L. McGreevy and L. Pusztai, *Mol. Simul.* **1**, 359 (1988).

- ³⁴<http://www.tagen.tohoku.ac.jp/general/building/iamp/database/scm/index.html>.
- ³⁵G. Kresse and J. Furthmüller, *Phys. Rev. B* **54**, 11169 (1996).
- ³⁶D. Vanderbilt, *Phys. Rev. B* **41**, 7892 (1990).
- ³⁷R. Busch, *J. Met.* **52**, 39 (2000).
- ³⁸S. M. Chathoth, A. Meyera, M. M. Koza, and F. Juranyi, *Appl. Phys. Lett.* **85**, 4881 (2004).
- ³⁹N. Mattern, H. Hermann, S. Roth, J. Sakowski, M.-P. Macht, P. Jovari, and J. Jiang, *Appl. Phys. Lett.* **82**, 2589 (2003).
- ⁴⁰Y. Waseda, *The Structure of Non-Crystalline Materials* (McGraw-Hill, New York, 1980).
- ⁴¹T. Egami, *Mater. Sci. Eng., A* **226–228**, 261 (1997).
- ⁴²D. B. Miracle, *Nature Mater.* **3**, 697 (2004).
- ⁴³W. L. Johnson, *Prog. Mater. Sci.* **30**, 81 (1986).
- ⁴⁴H. A. Davies and J. B. Hull, *J. Mater. Sci.* **11**, 215 (1976).
- ⁴⁵K. Tamura and H. Endo, *Phys. Lett.* **29A**, 52 (1969).
- ⁴⁶A. R. Yavari, *Nature (London)* **439**, 405 (2006).
- ⁴⁷D. B. Miracle, *Acta Mater.* **54**, 4317 (2006).
- ⁴⁸H. W. Sheng, W. K. Luo, F. M. Alamgir, J. M. Bai, and E. Ma, *Nature (London)* **439**, 419 (2006).
- ⁴⁹S. Ranganathan and A. Inoue, *Acta Mater.* **54**, 3647 (2006).
- ⁵⁰V. A. Shneidman and D. R. Uhlmann, *J. Chem. Phys.* **109**, 186 (1998).
- ⁵¹J. Schroers, Y. Wu, R. Busch, and W. L. Johnson, *Acta Mater.* **49**, 2773 (2001).
- ⁵²A. Takeuchi and A. Inoue, *Mater. Trans., JIM* **41**, 1372 (2000).
- ⁵³Z. P. Lu and C. T. Liu, *Acta Mater.* **50**, 3501 (2002).
- ⁵⁴X. H. Du, J. C. Huang, C. T. Liu, and Z. P. Lu, *J. Appl. Phys.* **101**, 086108 (2007).
- ⁵⁵T. Ichitsubo, E. Matsubara, H. Numakura, K. Tanaka, N. Nishiyama, and R. Tarumi, *Phys. Rev. B* **72**, 052201 (2005).
- ⁵⁶V. N. Novikov and A. P. Sokolov, *Nature (London)* **431**, 961 (2004).
- ⁵⁷O. N. Senkov, *Phys. Rev. B* **76**, 104202 (2007).